Ocean Sci. Discuss., 9, 2001–2038, 2012
www.ocean-sci-discuss.net/9/2001/2012/
doi:10.5194/osd-9-2001-2012

Ocean Science Discussions

Large-scale temperature and salinity changes in the upper Canadian basin of the Arctic Ocean at a time of a drastic Arctic Oscillation inversion

P. Bourgain[1], J. C. Gascard[1], J. Shi[2], and J. Zhao[2]

[1]LOCEAN, Université Pierre et Marie Curie, Paris, France
[2]College of Physical and Environmental Oceanography, Ocean University of China, Qingdao, China

Received: 2 April 2012 – Accepted: 5 April 2012 – Published: 10 May 2012

Correspondence to: P. Bourgain (pascaline.bourgain@locean-ipsl.upmc.fr)

Published by Copernicus Publications on behalf of the European Geosciences Union.

Abstract

Between 2008 and 2010, the Arctic Oscillation index over Arctic regions shifted from positive values corresponding to more cyclonic conditions prevailing during IPY period (2007–2008) to extremely negative values corresponding to strong anticyclonic conditions in 2010. In this context, we investigated the recent large scale evolution of the upper Western Arctic Ocean based on temperature and salinity summertime observations collected during icebreaker campaigns and from Ice-Tethered Platforms (ITP) drifting across the region in 2008 and 2010. Particularly, we focused on (1) the freshwater content which was extensively studied during previous years, (2) the Near Surface Temperature Maximum due to incoming solar radiation and (3) the water masses advected from the Pacific and Atlantic Oceans into the deep Arctic Ocean.

The observations revealed a freshwater content change in the Canadian basin during this time period. South of 80° N, the freshwater content increased, while north of 80° N, less freshening occurred in 2010 compared to 2008. This was more likely due to the strong anticyclonicity characteristic of a low AO index mode that enhanced both a wind-generated Ekman pumping in the Beaufort Gyre and a diversion of the Siberian rivers runoff toward the Eurasian basin at the same time.

The Near Surface Temperature Maximum due to incoming solar radiation was almost 1 °C colder in the Southern Canada basin (south of 75° N) in 2010 compared to 2008 which contrasted with the positive trend observed during previous years. This was more likely due to higher summer sea ice concentration in 2010 compared to 2008 in that region, and surface albedo feedback reflecting more sun radiation back in space.

The Pacific waters were also subjected to strong spatial and temporal variability between 2008 and 2010. In the Canada basin, both Summer and Winter Pacific waters influence increased between 75° N and 80° N. This was more likely due to a strong recirculation within the Beaufort Gyre. In contrast, south of 75° N, the PaW influence decreased indicative of the fact that they were not responsible for the freshening already mentioned, due to other sources. In addition, in the vicinity of the Chukchi Sea,

both Summer and Winter Pacific waters were significantly warmer in 2010 than in 2008 as a consequence of a general warming trend of the Pacific waters entering in the deep Arctic Ocean since 2008.

Finally, the warm Atlantic water remained relatively stable between 2008 and 2010 in the Canadian basin despite strong atmospheric shift, probably because of large time lag response. Atlantic water variability resulting from the presence of a warm "pulse-like" event in this region since 2005 was still noticeable even if a cooling effect was observed at a rate of $0.015\,^{\circ}\mathrm{C\,yr^{-1}}$ between 2008 and 2010 in that region.

1 Introduction

Over the past decade, the most intense changes of the Arctic summer sea ice cover occurred in the Canadian basin strongly affecting the exchanges between the ocean and the atmosphere in this region.

Additionally, between 2008 and 2010, the Arctic atmospheric forcing changed drastically. Following a period of positive phase of the Arctic Oscillation (AO) ending in 2008, the AO reached the lowest value in 2010 since 1950 (see Fig. 1). This recent evolution of the AO corresponds to one of the most abrupt shift over the last decades. It is comparable in magnitude (but opposite in sign) to the shift observed in the late 1980s which was responsible for some major changes in sea-ice advection (Kwok, 2000; Rigor et al., 2002) and oceanic circulation (for overview see Dickson et al., 2000) in the Arctic Ocean with consequences on the Northern Atlantic deep convection (Gerdes et al., 2008).

In such a context, what could be the response of the Arctic Ocean to the drastic increase of the atmospheric anticyclonicity and changes in the sea ice cover? The ocean interior might respond slowly to these new forcing conditions due to long time scale related to baroclinic transport (Morison et al., 2006) but what about the upper ocean?

We propose to analyse the recent evolution of the upper ocean water masses in the Canadian basin, based on CTD observations collected in this region during the summers 2008 and 2010. After presenting the data set, we will analyse the short-term variability of the main oceanic features of the Canadian basin upper ocean in light of the recent changes in the atmosphere and in the sea ice.

2 Data and method

2.1 Presentation of the area

Based on the bathymetry, the Canadian basin is subdivided into different areas (see Fig. 2). The vast ($\sim$ 800 km in meridional extent) and shallow (< 100 m) Chukchi shelf is edged by a continental slope in the North and an abrupt shelf-break in the North-East. The Chukchi Borderland (ChB), considered as a mid-depth (1000 m) extension of the Chukchi shelf, is a complex area composed by the Chukchi Abyssal Plain (CAP), the 200 km long Chukchi Plateau (CP) separated from the Chukchi shelf by the Chukchi Gap, and the Northwind Ridge (NR). One of the possible gateway for the Chukchi shelf waters to enter the deep Arctic Ocean is north of the Alaskan coast, through the Barrow Canyon (BA area). Close to the Canadian Archipelago, the Mackenzie River provides freshwater to the shelves (MK area). The deep basins (1000 m to 4000 m) are composed of the Canada Abyssal Plain or Canada basin (CaB) and the Mendeleyev Abyssal Plain (MAP). These deep basins are separated from the Makarov basin (MaB) by the Alpha Ridge (AR) on the East and by the Mendeleyev ridge (MR) on the West.

In the following, we will focus our analysis on five main areas of the Canadian side of the Arctic Ocean (located by ellipses on Fig. 2): the Chukchi borderland (ChB including the CP, the NR and the CAP), the Barrow canyon region (BA) and the Mackenzie River region (MK) for the relatively shallow regions, and the Canada basin (CaB) and the Mendeleyev Abyssal Plain (MAP) for the deep basins. These five areas cover the main regions of the Canadian basin of the Arctic Ocean, providing some representation of the overall situation in this basin. Note that the regional means will be sometimes associated with large standard deviations due to the heterogeneity of a variable inside a same region.

2.2 Data

A high number of CTD measurements were collected during the CHINARE 2008 and 2010 campaigns (July-August-September) on board the Chinese icebreaker Xuelong: 88 and 143 CTD were collected in 2008 and 2010, respectively, in the Bering Sea, the Chukchi Sea and in the Arctic Ocean. In this paper, we will focus on CTD stations realized north of 70° N and deeper than 50 dbar. For both campaigns, the CTD was a SBE 9 mounted on a 24-bottles rosette sampler with 10 l Niskin Bottles. Accuracy of temperature and conductivity measurement was 0.001 °C and 0.0003 $\mathrm{S\,m^{-1}}$, respectively. The SBE 9 CTD was calibrated before and after the campaigns. In 2010, the summer ice conditions in the Northern Canadian basin were light and the icebreaker was able to go as far north as 88.4° N compared to 85.4° N in 2008.

The data set collected during CHINARE campaigns in the Canada basin in summers 2008 and 2010 was completed with data collected in the same area during other icebreaker campaigns (Table 1 and Fig. 3): the RV-Polarstern ARK XXIII/3 cruise (September 2008) and the CCGS Louis S. St-Laurent (LSSL) campaigns (July-August 2008 and September-October 2010). In addition, we also used data collected by drifting buoys, the Ice-Tethered Profilers (ITP-1 profile on 10-July to mid October 2008 and 2010), deployed by the WHOI.

2.3 Methodology

After removing outliers, the data set, extending from near surface down to 1000 decibar (dbar) level, was interpolated each 1 dbar. The density and the potential temperature were calculated using UNESCO 1983 tables. Raw gradients were obtained from the differences between two successive values sampled 1 dbar apart.

OSD
9, 2001–2038, 2012

We used the Kriging interpolation method to construct spatial maps on a 1° longitude × 0.5° latitude grid of several parameters first estimated from original T and S profiles. The Kriging method is a geostatistical technique to interpolate the value of a random field from observations at nearby locations that improves over all other interpolation methods because it minimizes error covariance. We chose the ten closest points within a certain radius to be the Kriging interpolation neighbourhood. The minimum radius was determined by the range of the variogram (Krige, 1951; Matheron, 1963), around 300 km.

In this paper, we focused on large-scale changes from 2008 to 2010. However, because some of the data were collected either at the beginning or at the end of the summer season (for instance, LSSL 2008 was realized in July-August while LSSL 2010 was realized in September-October), seasonal variability might intervene in the differences observed from one year to another.

3 Regional hydrography and recent changes

The Canadian basin water column structure (see Fig. 4) is more complex than in the Eurasian basin due to the presence of different temperature extrema between the surface mixed layer and the thermocline: First, located immediately below the surface mixed layer, the Near Surface Temperature Maximum (NSTM) is due to incoming solar radiation (Jackson et al., 2010). Then, the Summer Pacific water (SPaW) is located at 50–80 m depth, in the upper halocline, and finally, the Winter Pacific water (WPaW) is located in the middle halocline, above the thermocline. At greater depth (300–500 m depth), the warm and salty Atlantic waters (AW) constitute the main reservoir of heat for the whole Arctic Ocean.

3.1 The NSTM

3.1.1 Background

Jackson et al. (2010) have shown that in the Central Canadian basin, the ice free upper ocean layer being in direct contact with the atmosphere and exposed to incoming solar radiation has the capacity to store heat. A shallow seasonal halocline due to sea ice melt may isolate the surface layer warmed up by incoming solar radiation. This creates a Near Surface Temperature Maximum (NSTM) located typically at depths of 25–35 m (above the Summer Pacific water) and at salinities less than 31 psu. This heat can be stored year-round in the Canada basin if the summer halocline persists throughout the year (Jackson et al., 2010).

When looking at AIDJEX (Arctic Ice Dynamics Joint Experiment) profiles acquired in 1975, Toole et al. (2010) noticed that there was "virtually no NSTM" in the Canada basin water column at this time. More recently, Jackson et al. (2010) observed that the NSTM increased and moved northward and upward from 1993 to 2007. Between 75° N and 80° N, the extreme NSTM values were observed in 2007 (maximum) and in 2003–2004 (minimum), which corresponds to an increasing rate of 0.13 $^{\circ}\mathrm{C\,yr}^{-1}$ from 2004 to 2007. In addition, the NSTM shoaled by 2.1 $\mathrm{m\,yr}^{-1}$ since 1997 when the NSTM was the deepest, at about 33 m depth, to reach 15 m depth in 2007. Jackson et al. (2010) suggested that the NSTM increase was linked to sea ice melt. During the extreme sea ice retreat of summer 2007, Ice Mass Balance (IMB) buoys recorded an exceptional large amount of ice bottom melting in the Beaufort Sea region associated to a 500 % positive anomaly in solar heat input to the upper ocean (Perovich et al., 2008), highlighting the importance of the NSTM in the sea ice mass balance.

3.1.2 New results

Applying Jackson et al.'s definition for the NSTM, we observed in 2008 and 2010 that the highest temperatures were located in the Southern Canadian basin, close to the

Alaskan coasts (Fig. 5). In some regions of the Northern Canadian basin, there was no NSTM evidenced (grey areas on Fig. 5). Note that some profiles did not reach the surface and may have not sampled the NSTM for this reason.

From 2008 to 2010, we observed a general decrease and deepening of the NSTM in the Canadian basin, south of 80° N, which contrast with the situation of the previous years as described by Jackson et al. (2010). For instance, in the ChB, the NSTM decreased by -0.77 ± 0.68 °C and deepened by 5 ± 8 dbar (Table 2). In the Southern CaB, the NSTM was particularly smaller (by more than 1 °C) and deeper (by more than 10 dbar) in 2010 compared to 2008. Note that at some locations in the BA and MK, there was a strong NSTM increase but more data would be needed to confirm it.

Arctic sea ice concentrations were relatively similar at the end of the melt season (September) in 2010 and 2008 (Stroeve et al., 2011). However, noticeable differences between the two years appeared in the Southern Canadian basin with more sea ice in 2010. When analysing sea ice motion fields, Stroeve et al. (2011) observed a strengthening of the southward and westward transport of sea ice due to wind forcing along the Canadian Archipelago towards the Eastern Beaufort Sea. The sea ice transport was 124 % higher than climatology in this region. As a result, the 2010 melt season started with an area of multiyear ice extending from the Beaufort Sea into the Chukchi Sea, which contrasted with the situation observed in 2008 and 2009. With more sea ice resulting into less open water areas, less incoming solar radiation could penetrate into the upper ocean through open water areas and/or leads to warm up the surface layers, resulting into a smaller NSTM. Therefore, the sea ice concentration increase between 2008 and 2010 in the Southern Canadian basin, due to enhanced transport from the Canadian Archipelago (Stroeve et al., 2011), was more likely responsible for the strong NSTM decrease (by more than 1 °C in the Southern CaB) observed in the same region. We agree with Jackson et al. (2010) when suggesting that the sea ice concentration could be a major driver of the NSTM variability.

3.2 The Pacific waters

3.2.1 Background

The major distinction between the upper water columns of the Canadian and Eurasian basins is related to the presence or not of Pacific waters (PaW), an important source of nutrients and of freshwater for the Arctic Ocean (Woodgate and Aagaard, 2005). These waters enter through Bering Strait and then transit in the Chukchi Sea for several months (Woodgate et al., 2005a) before entering the deep Arctic Ocean.

The PaW are strongly affected by seasonal processes. In winter, cooling and sea ice production release brines in the water column and contribute to a colder and saltier Pacific water mass than during summertime. As a consequence, this winter Pacific water (WPaW, sometimes referred to as the winter Bering Sea Water like in Coachman and Barnes, 1961) is characterized by a minimum of temperature at greater salinities and at greater depth than the summer Pacific water (SPaW), characterized by a temperature maximum at relatively low salinities (between 31 psu and 33 psu). In addition to the strong seasonal signal observed in the Bering Strait (Woodgate et al., 2005b), the PaW are modified in winter during their transit in the Chukchi Sea depending on the fall and winter conditions which control seasonal ice development (Weingartner et al., 2005). When entering the deep Arctic basin, the SPaW and WPaW influence the upper part and the middle part of the halocline, respectively (McLaughlin et al., 2004). As a result, the "double halocline structure" (Shimada et al., 2005; Shi et al., 2005) characteristic of the Canadian basin, is different from the "cold halocline" encountered in the Eurasian basin (Aagaard et al., 1981).

Observations led by Woodgate et al. (2010) in the Bering Strait revealed an annual mean rise of temperature of SPaW from $-0.4\,^{\circ}$C in 2001 to $+0.4\,^{\circ}$C in 2007. Other observations (Bourgain and Gascard, 2012) indicated that the SPaW was particularly warm in the Canadian basin during the IPY compared to the previous decade.

3.2.2 New results

The Summer Pacific water

The influence of the SPaW, defined as a temperature maximum located below 40 dbar within the salinity range (31 psu 33 psu), is quantified by the index PWI which is the difference between the temperature maximum and the corresponding freezing point (Bourgain and Gascard, 2012).

Between 75° N and 80° N, the SPaW warmed up from 2008 to 2010 in the Canadian basin: In the Northern CaB in particular, it warmed up by more than 0.3 °C and shoaled by 5–10 dbar (Table 3, Fig. 6) for which possible explanation is proposed in Sect. 3.4.2. By contrast, in the Southern Canadian basin (Southern CaB and MK, corresponding to the Beaufort Sea), the SPaW strongly cooled down (by -0.50 ± 0.23 °C in MK). Finally, in BA, there was a particularly strong warming of 0.35 ± 0.43 °C between 2008 and 2010. Note that the SPaW could have moved back from the north east of the MAP (Fig. 6, grey areas), but the absence of observations in 2010 in this area (see Fig. 3) did not allow to rely on the Kriging interpolation process (high uncertainties associated) and the results in this region were not reliable.

The Winter Pacific water

We used the definition proposed by Pickart et al. (2005) for characterizing the WPaW: a water mass with a salinity above 32.4 psu and a temperature below −1.4 °C. When available, nutrients are useful tracers for this water mass taking into account the fact that the WPaW is nutrients rich due to a reduced biological production on the Chukchi shelf in wintertime (Ekwurzel et al., 2001). Silicate concentration measured during the CHINARE 2008 cruise indicated that the WPaW did not extend further north than 86° N (Coupel et al., 2011). Therefore and since we did not take into account nutrients in our WPaW index definition, we will not rely on the results of the WPaW index north of 86° N based on this definition.

OSD
9, 2001–2038, 2012

From 2008 to 2010, the WPaW temperature decreased significantly in the CaB, especially north of 75° N, with a cooling greater than 0.05 °C and a deepening of 20 dbar minimum (see Fig. 7). This adds up to a warming of the SPaW observed in the same area (see "The Summer Pacific water"), indicating a general increasing influence of the PaW in this region for which explanations will be proposed in Sect. 3.4.2.

Between 2008 and 2010, the WPaW warmed up in MK and south of CaB. Together with the cooling of the SPaW in the same region, this suggests a general decreasing influence of the PaW in the Beaufort Sea which follows a trend initiated a few years before (see Bourgain and Gascard, 2012, Fig. 5). Indeed, Morison et al. (2012) estimated that the PaW fraction of freshwater decreased by 0.8 m (relative to the salinity 34.87psu) in this region between 2005 and 2008.

Observations also revealed that the regions located in the vicinity of the Chukchi Sea (BA, south of ChB) evidenced a warming of WPaW in 2010 compared to 2008. Such a warming, together with the SPaW warming observed in the same region (see "The Summer Pacific water"), indicates a general warming trend of the PaW penetrating the deep Arctic Ocean since 2008. Upstream observations would be needed to determine if these PaW acquired this extra heat during their transit on the Chukchi shelf or if they captured it before.

3.3 The Atlantic water

3.3.1 Background

The warm and salty Atlantic waters (AW) enter the Arctic Ocean through Fram Strait (the Fram Strait Branch) and the Barents Sea (the Barents Sea branch) and are located in the water column between 300–700 m depth. The Barents Sea branch, colder than the Fram Strait Branch, is located deeper in the water column (Rudels et al., 1994; Schauer et al., 1997). From the Eurasian basin to the Canadian basin, the AW is transported by topographically steered boundary currents at a speed of 1–2 $cm\,s^{-1}$

(Woodgate et al., 2001). In this study, we will focus on the Fram Strait branch component of the AW identified by the AW maximum temperature.

In addition to long-term variability (Polyakov et al., 2004), warm AW "pulse-like" events exist and can be detected upstream as far as in the Norwegian Atlantic current and in the sub-polar basins (Orvik and Skagseth, 2005; Polyakov et al., 2005). The first observation of a warm "pulse-like" event was realised in the 1990s when positive AW temperature anomalies of up to 1 °C relative to the 1970s temperatures were measured throughout over vast areas of the Eurasian and Makarov Basins (Quadfasel et al., 1991; Carmack et al., 1995; Swift et al., 1997; Morison et al., 1998; Steele and Boyd 1998; Polyakov et al., 2004). More recently, another warm AW pulse of about 0.8 °C first observed East of Svalbard in 2004 (Polyakov et al., 2005) propagated along the continental slope of the Eurasian basin in the late 2000s (Ivanov et al., 2009; Bourgain and Gascard, 2012). In the Canadian basin, remnants of the historical signal first observed by Quadfasel et al. (1991) were detected in the northern and western side of the Chukchi Plateau in the early 2000s (McLaughlin et al., 2004; Shimada et al., 2004) and in the Central Canada basin in 2005 (Bourgain and Gascard, 2012), corresponding to a travel time of about 15 yr from Fram Strait. Additional data indicate that from the time period 2003–2006 to 2007–2008, this historical "pulse-like" signal cooled down at a rate of $-0.017\,^{\circ}\mathrm{C\,yr^{-1}}$ in the CaB and $-0.018\,^{\circ}\mathrm{C\,yr^{-1}}$ in the ChB.

3.3.2 New results

Our recent observations revealed that the warm historical AW "pulse-like" that arrived in the Canada basin in 2005 (Bourgain and Gascard, 2012) kept cooling in CaB and ChB, between 75° N and 80° N after 2008 at a comparable rate than previous years with a cooling ranging from −0.02 °C to −0.04 °C over the two years (Table 5 and Fig. 8). This suggests that the warm anomaly or "pulse-like" gradually vanished by cooling due to contact with colder surrounding waters.

Discussion Paper | Discussion Paper | Discussion Paper | Discussion Paper |

OSD

9, 2001–2038, 2012

Hydrographic changes in the Canadian basin during AO inversion

P. Bourgain et al.

In addition, the northern part of MAP could have experienced a warming of the AW but the absence of data in this area in 2010 does not permit to rely on the Kriging interpolation process.

3.4 The freshwater content

3.4.1 Background

Pacific waters and river runoff are the primary sources of freshwater in the Arctic Ocean (Jones et al., 2008; McPhee et al., 2009), providing a total input of 8500 $km^3 yr^{-1}$ with a mean residence time of about a decade. About 45 000 km^3 of freshwater (relative to the salinity $S = 34.8$ psu), representing 60 % of the total oceanic freshwater content of the Arctic Ocean, is stored in the Beaufort Gyre, an extensive anticyclonic gyre in the Canada basin north of Alaska (Aagaard and Carmack, 1989; Serreze et al., 2006).

Recent observations indicated a substantial freshening in the Canada and Makarov basins (Mc Phee et al., 2009; Rabe et al., 2011). Proshutinsky et al. (2009) estimated the freshwater content positive trend to be 178 $cm\,yr^{-1}$ (when calculated with $S = 34.8$ psu as the reference salinity) south of 80° N for the 2003–2007 time period. Bourgain and Gascard (2011) observed an intensification of the surface salinity freshening in 2007–2008. The Siberian river runoff pathways (Morison et al., 2012) or the strength of the Beaufort Gyre (Giles et al., 2012) have a major influence on the freshwater content variability.

3.4.2 New results

We used the method described in Rabe et al. (2011) to obtain the inventory of liquid freshwater H_{FW} between the surface and the 34 isohaline depth. It is given in meters by:

$$H_{FW} = \int (S_{ref} - S)/S_{ref} dz$$

OSD
9, 2001–2038, 2012

with S, the observed salinity, and $S_{ref} = 35$ psu.

For both years (2008 and 2010), the maximum of H_{FW} was located in the Beaufort Sea (Fig. 9). This was due to the persistent anticyclonic wind pattern, leading to Ekman pumping and an accumulation of freshwater in the Beaufort Gyre. In addition, there was a gradual decline of H_{FW} from the Beaufort Sea toward the Siberian shelf seas and toward North Pole during both years (see Table 6). Our results for year 2008 are in good agreement with Rabe et al. (2010) observations for 2006–2008 time period with H_{FW} reaching more than 25 m in the Beaufort Gyre and minimum values (between 6m and 13 m) encountered in the Western MAP.

We estimated that H_{FW} increased in the CaB and in the ChB by 1.89±1.35 m between 2008 and 2010 (Table 6). Proshutinsky et al. (2010) observations indicated that the H_{FW} increase in ChB did occur since 2009. In the southern regions, H_{FW} decreased by 3.52 m in MK and increased by 3.04 m in BA from 2008 to 2010. Northward, in the MAP, H_{FW} decreased by 2.78 m on average but the high standard deviation indicates large spatial heterogeneity within this region and Fig. 9 suggests that the decrease may be much stronger in the Northern MAP. When calculating the average evolution of the liquid freshwater content (= H_{FW} × surface area) in the five different regions from 2008 to 2010, we found a decrease of 1256 ± 1437 km^3 in the MAP and an increase of 752±537 km^3 in the CaB. In the shallow regions, we obtain an increase of 870±626 km^3 and 317 ± 132 km^3 in the ChB and BA, respectively and a decrease of 845 ± 336 km^3 in the MK.

Compared to previous years, our results suggested that the Southern Canadian basin kept accumulating freshwater between 2008 and 2010 (except in MK) while the Northern Canadian basin underwent a small decrease in its liquid freshwater inventory following a strong surface waters freshening during IPY years (Bourgain and Gascard, 2011).

Proshutinsky et al. (2002, 2009) and Condron et al. (2008) have shown that decadal variations of the freshwater content in the Beaufort Gyre were associated with changes in atmospheric forcing. When anticyclonic wind conditions prevail, the freshwater content increases in the Beaufort Gyre as a result of the enhanced wind-generated Ekman Pumping, and vice-versa. Therefore, the strong anticyclonic wind conditions characterizing the summer 2010 are more likely responsible for the observed freshwater content increase of $752 \pm 537\,km^3$ in the CaB between 2008 and 2010.

In adecuation with this hypothesis, Steele et al. (2004) proposed that during negative AO phases, one of the main sources of freshwater, the PaW, strongly recirculates within the Beaufort Gyre. As a consequence, the extreme increase in atmospheric anticyclonicity in 2010, characterized by a smaller transport in the transpolar drift (61 % less) than climatology and a strong Beaufort Sea High (Stroeve et al., 2011), most likely explains why there are more PaW between 75° N and 80° N in CaB (see Sect. 3.2.2), which contributes as a result, to the freshwater content increase observed in this region. In contrast, south of 75° N, the concomitant PaW influence decrease and freshwater content increase indicates that other sources than PaW intervene in the more intense surface freshening water of this region. Cause of the PaW influence decrease south of 75° N in CaB remains to be determined.

The less freshening of the northern part of MAP may be explained in terms of decreasing Siberian river runoff input. The diversion of the Siberian rivers runoff in the Arctic Ocean is strongly affected by the wind forcing (Johnson and Polyakov, 2001; Morison et al., 2012) with anticyclonic conditions driving the river runoff toward the Amundsen basin rather than toward the Makarov basin and the Northern Canadian basin. This is opposed to what occurred during the early 1990s (Steele and Boyd, 1998) or the late 2000s (Bourgain and Gascard, 2011) when cyclonic conditions prevailed.

4 Conclusions

We investigated the large scale changes of the Canadian basin water column based on summertime observations from 2008 and 2010 at a time of a strong AO inversion.

OSD
9, 2001–2038, 2012

Following positive AO index in 2008, the extreme low index of AO in 2010, a sharp increase of the atmospheric anticyclonicity, was responsible for the large scale freshwater content change observed in the Canadian basin. North of 80° N, anticyclonic winds driving the Siberian river runoff toward the Eurasian basin induced less freshening in the Northern MAP between 2008 and 2010, in contrast with IPY years characterized by more cyclonic conditions and strong surface waters freshening in that region. Strikingly, in the Beaufort Gyre (CaB), the freshwater content increased by up to $752 \pm 537\,\mathrm{km}^3$ from 2008 to 2010, more likely due to enhanced wind-generated Ekman Pumping.

Following a positive trend of $+0.13\,^{\circ}\mathrm{C\,yr}^{-1}$ observed from 2004 to 2007 in the Canada Basin (Jackson et al., 2010), the NSTM decreased by almost 1 °C south of 75° N between 2008 and 2010, more likely due to a surface albedo feedback related to a sea ice concentration increasing in the Beaufort Sea from 2008 to 2010 (Stroeve et al., 2011).

In the Canada basin, the PaW evidenced different behaviour south and north of 75° N between 2008 and 2010. From 2008 to 2010, and between 75° N and 80° N, the PaW influence increased (The SPaW warmed up and the WPaW cooled down) possibly due to the strong recirculation within the Beaufort Gyre during negative AO index phase as proposed by Steele et al. (2004). In contrast, PaW influence decreased south of 75° N from 2008 to 2010 (The SPaW cooled down and the WPaW warmed up), following a tendency identified since 2005 (Morison et al., 2012; Bourgain and Gascard, 2012) but for unknown reasons. In regions located in the vicinity of the Chukchi Sea (BA, Southern ChB), the PaW (both Summer and Winter waters) warmed up significantly, which indicates a general warming trend of the PaW entering in the deep Arctic Ocean since 2008. Was this extra heat carried out from Bering Strait as partly suggested by Woodgate et al. (2010) up to 2008, and/or acquired when transiting across the Chukchi shelf remains to be answered.

South of 80° N, the warm AW "pulse-like" anomaly observed in 2005 in the Canada basin (Bourgain and Gascard, 2012) 15 yr after it was first observed in the Nansen basin (Quadfasel et al., 1991), cooled off between 2008 and 2010 due to normal heat exchange with cold surrounding waters. Besides this observation, the AW in the

Canadian basin remained quite stable from 2008 to 2010. However, because the ocean interior might respond with a significant time lag to extreme increase of atmospheric anticyclonicity due to long time transport and slow baroclinic motion (Morison et al., 2006), major oceanic changes are expected within the next few years in response to the 2010 AO index lowest record.

Acknowledgements. We express our gratitude to the captain and the crew of the Xuelong icebreaker for the opportunity to take part in the field work in the Arctic Ocean. We thank the Second Institute of Oceanography SOA/PRC (State Oceanic Administration, China, Hangzhou) to invite the French scientists from the LOCEAN laboratory (UPMC-University Pierre et Marie Curie) to participate to the CHINARE cruise. The Ice-Tethered Profiler data were collected and made available by the Ice-Tethered Profiler Program based at the Woods Hole Oceanographic Institution (http://www.whoi.edu/itp). Polarstern data come from the DAMOCLES project financed by the European Union in the 6th Framework Programme for Research and Development. We are grateful to Sarah Zimmerman for the LSSL data. We thank Pierre Coupel for helpful discussion. Finally, we are very grateful to the Geovariances compagy for advises and help about the Kriging interpolation theory and process on ISATIS software. The PhD was supported by the AXA Research Fund.

INSU
Institut national des sciences de l'Univers

The publication of this article is financed by CNRS-INSU.

References

Aagaard, K. and Carmack, E. C.: The role of sea ice and other fresh water in the arctic circulation, J. Geophys. Res., 94(10), 14485–14498, 1989.

Aagaard, K., Coachman, L. K., and Carmack, E.: On the halocline of the Arctic Ocean, Deep-Sea Res. Pt. A, 28, 529–545, 1981.

Beal, M. A., Edvalson, F., Hunkins, K., Molloyl, A., and Ostenso, N.: The floor of the Arctic Ocean: Geographic names, ARCTIC: Journal of the Arctic Institute of North America, The Arctic Institute of North America, 19(3), 213–284, 1966.

Bourgain, P. and Gascard, J. C.: The Arctic Ocean halocline and its interannual variability from 1997 to 2008, Deep-Sea Res. Pt. I, 58, 745–756, 2011.

Bourgain, P. and Gascard, J.C: The Atlantic and Summer Pacific waters variability in the Arctic Ocean from 1997 to 2008, Geophys. Res. Lett., 39, L05603, doi:10.1029/2012GL051045, 6 pp., 2012.

Carmack, E., Macdonald, R., Perkin, R., McLaughlin, F., and Pearson, R.: Evidence for Warming of Atlantic Water in the Southern Canadian Basin of the Arctic Ocean: evidence from the Larsen-93 Expedition, Geophys. Res. Lett., 22, 1061–1065, 1995.

Coachman, L. K. and Barnes, C. A.: The Contribution of Bering Sea Water to the Arctic Ocean, Number 249 from the Department of Oceanography, University of Washington, 1961.

Condron, A., Winsor, P., Hill, C., and Menemenlis, D.: Simulated response of the arctic freshwater budget to extreme NAO wind forcing, J. Climate, 22, 2422–2437, doi::10.1175/2008JCLI2626.1, 2009.

Coupel, P., Jin, H. Y., Ruiz-Pino, D., Chen, J. F., Lee, S. H., Li, H. L., Rafizadeh, M., Garçon, V., and Gascard, J. C.: Phytoplankton distribution in the Western Arctic Ocean during a summer of exceptional ice retreat, Biogeosciences Discuss., 8, 6919-6970, doi:10.5194/bgd-8-6919-2011, 2011.

Dickson, R. R., Meincke, Malmberg, S. A., and Lee, A. J.: The “Great Salinity Anomaly” in the northen North Atlantic 1968–1982, Prog. Oceanogr., 20, 103–151, 1988.

Dickson, R. R., Osborne, T. J., Hurrell, J. W., Meincke, J., Blindheim, J., Adlandsvik, B., Vinje, T., Alekseev, G., and Maslowski, W.: The Arctic Ocean response to the North Atlantic oscillation, J. Climate, 13, 2671–2696, 2000.

OSD

9, 2001–2038, 2012

Hydrographic changes in the Canadian basin during AO inversion

P. Bourgain et al.

Ekwurzel, B., Schlosser, P., Mortlock, R. A., and Fairbanks, R. G.: River runoff, sea ice meltwater, and Pacific water distribution and mean residence times in the Arctic Ocean, J. Geophys. Res., 106(C5), 9075–9092, 2001.
Gerdes, R., Karcher, M., Köberle, C., and Fieg, K.: Simulating the long term variability of liquid freshwater export from the Arctic Ocean , Arctic-Subarctic Ocean Fluxes: Defining the role of the Northern Seas in Climate, edited by:: Dickson, B., Meincke, J., and Rhines, P., Springer, ISBN: 978-1-4020-6773-0, 2008.
Giles, K. A., Laxon, S. W., Ridout, A. L., Wingham, D. J., and Bacon, S.: Western Arctic Ocean freshwater storage increased by wind-driven spin-up of the Beaufort Gyre, Nat. Geosci., 5, 194–197; doi:10.1038/ngeo1379, 2012.
Ivanov, V. V., Polyakov, I. V., Dmitrenko, I. A., Hansen, E., Repina, I. A., Kirillov, S. A., Mauritzen, C., Simmons, H., and Timokhov, L. A.: Seasonal oceanic variability off Svalbard in 2004–06, Deep-Sea Res. Pt. I, 56, 1–14, 2009.
Jackson, J. M., Carmack, E. C., McLaughlin, F. A., Allen, S. E., and Ingram, R. G.: Identification, characterization, and change of the near-surface temperature maximum in the Canada Basin, 1993–2008, J. Geophys. Res., 115(C0), 5021, 2010.
Johnson, M. A. and Polyakov, I. V.: The Laptev Sea as a source for recent Arctic Ocean salinity changes, Geophys. Res. Lett., 28(10), 2017–2020, 2001.
Jones, E. P., Anderson, L. G., Jutterström, S., Mintrop, L., and Swift, J. H.: Pacific freshwater, river water and sea ice meltwater across Arctic Ocean basins: Results from the 2005 Beringia Expedition, J. Geophys. Res., 113(C8), 1–10, 2008.
Krige, D. G.: Une approche statistique à quelques évaluations de mine et problèmes alliés chez le Witwatersrand, Thèse principale de l'université de Witwatersrand, 1951.
Kwok, R.: Recent changes in Arctic Ocean sea ice motion associated with the North Atlantic Oscillation, Geophys. Res. Lett., 27(6), 775–778, 2000.
Matheron, G.: Principes de geostatistics, Geol. Econom., 58, 1246–1266, 1963.
McLaughlin, F. A., Carmack, E. C., and Macdonald, R. W.: Physical and geochemical properties across the Atlantic/Pacific water mass front in the Southern Canadian basin, J.Geophys. Res., 101(C1), 1183–1197, 1996.
McLaughlin, F. A., Carmack, E. C., Macdonald, R. W., Melling, H., Swift, J. H., Wheeler, P. A., Sherr, B. F., and Sherr, E. B.: The joint roles of Pacific and Atlantic origin waters in the Canada basin 1997–1998, Deep-Sea Res. Pt. I, 51, 107–128, 2004.

McPhee, M. G., Proshutinsky, A., Morison, J. H., Steele, M., and Alkire, B.: Rapid change in freshwater content of the Arctic Ocean. Geophys. Res. Lett., 36, L10602, doi:10.1029/2009GL037525, 2009.

Morison, J. H., Steele, M., and Andersen, R.: Hydrography of the upper Arctic Ocean measured from the nuclear submarine USS Pargo, Deep-Sea Res. Pt. I, 45, 15–38, 1998.

Morison, J., Steele, M., Kikuchi, T., Falkner, K., and Smethie, W.: Relaxation of Central Arctic Ocean hydrography to pre-1990s climatology, Geophys. Res. Lett., 33, L17604, doi:10.1029/2006GL026826, 2006.

Morison, J. H., Kwok, R., Peralta-Ferriz, C., Alkire, M., Rigor, I., Andersen, R., and Steele, M.: Changing Arctic Ocean freshwater pathways, Nature, 481, 66–70, doi:10.1038/nature10705, 2012.

Orvik, K. A. and Skagseth, O.: Heat flux variations in the Eastern Norwegian Atlantic current toward the Arctic from moored instruments, 1995–2005, Geophys. Res. Lett, 32, L14610, doi:10.1029/2005GL023487, 2005.

Perovich, D. K., Richter-Menge, J. A., Jones, K. F., and Light, B.: Sunlight, water, and ice, 2008, Extreme Arctic sea ice melt during the summer of 2007, Geophys. Res. Lett., 35, L11501, doi:10.1029/2008GL034007, 2008.

Pickart, R. S., Weingartner, T. J., Pratt, L. J., Zimmermann, S., and Torres, D. J.: Flow of winter-transformed Pacific water into the Western Arctic, Deep-Sea Res. Pt. II, 52, 3175–3198, 2005.

Polyakov, I. V., Alekseev, G. V., Timokhov, L. A., Bhatt, U. S., Colony, R. L., Simmons, H. L., Walsh, D., Walsh, J. E., and Zakharov, V. F.: Variability of the intermediate atlantic water of the Arctic Ocean over the last 100 years, J. Climate, 17, 4485–4497, doi:http://dx.doi.org/10.1175/JCLI-3224.1, 2004.

Polyakov, I. V., Beszczynska, A., Carmack, E. C., Dmitrenko, I. A., Fahrbach, E., Frolov, I. E., Gerdes, R., Hansen, E., Holfort, J., Ivanov, V. V., Johnson, M. A., Karcher, M., Kauker, F., Morison, J., Orvik, K. A., Schauer, U., Simmons, H. L., Skagseth, O., Sokolov, V. T., Steele, M., Timokhov, L. A., Walsh, D., and Walsh, J. E.: One more step toward a warmer Arctic, Geophys. Res. Lett., 32, L17605, doi:10.1029/2005GL023740, 2005.

Polyakov, I. V., Timokhov, L. A., Alexeev, V. A., Bacon, S., Dmitrenko, I. A., Fortier, L., Folov, I. E., Gascard, J. C., Hansen, E., Ivanov, V. V., Laxon, S., Mauritzen, C., Perovich, D., Shimada, K., Simmons, H. L., Sokolov, V. T., Steele, M., and Toole, J.: Arctic

Ocean warming contributes to reduced polar ice cap, J. Phys. Oceanogr., 40, 2743–2756. doi:http://dx.doi.org/10.1175/2010JPO4339.1, 2010.
Proshutinsky, A., Bourke, R. H., and McLaughlin, F. A.: The role of the Beaufort Gyre in Arctic climate variability: seasonal to decadal climate scales, Geophys. Res. Lett., 29, 2100, doi:10.1029/2002GL015847, 2002.
Proshutinsky, A., Krishfield, R., Timmermans, M.-L., Toole, J., Carmack, E., McLaughlin, F., Williams, W. J., Zimmermann, S., Itoh, M., and Shimada, K.: Beaufort Gyre freshwater reservoir: state and variability from observation, J. Geophys. Res., 114, C00A10, 25 pp., doi:10.1029/2008JC005104, 2009.
Proshutinsky, A., Timmermans, M. L., Ashik, I., Beszczynska- Moeller, A., Carmack, E., Frolov, I., Krishfield, R., McLaughlin, F., Morison, J., Polyakov, I., Shimada, K., Sokolov, V., Steele, M., Toole, J., and Woodgate, R.: Ocean [in Arctic Report Card 2010], available at: http://www.arctic.noaa.gov/reportcard, 2010.
Quadfasel, D. A., Sy, A., Wells, D., and Tunik, A.: Warming in the Arctic, Nature, 350, 385, doi:10.1038/350385a0, 1991.
Rabe, B., Karcher, M., Schauer, U., Toole, J. M., Krishfield, R. A., Pisarev, S., Kauker, F., Gerdes, R., and Kikuchi, T. : An assessment of Arctic Ocean freshwater content changes from the 1990s to the 2006–2008 period, Deep-Sea Res. Pt. I, 58, 173–185, 2011.
Rigor, I. G., Wallace, J. M., and Colony, R. L.: Response of sea ice to the Arctic Oscillation, J. Climate, 15, 2648–2663, 2002.
Rudels, B., Jones, E. P., Anderson, L. G., and Kattner, G.: On the intermediate depth waters of the Arctic Ocean, in: The Polar Oceans and Their Role in Shaping the Global Environment, Geophys. Monogr. Ser., vol. 85, edited by: Johannessen, O. M., Muench, R. D., and Overland, J. E., AGU, Washington, DC, 33–46, 1994.
Schauer, U., Muench, R. D., Rudels, B., and Timokhov, L.: Impact of Eastern Arctic shelf waters on the Nansen Basin intermediate layers, J. Geophys. Res., 102, 3371–3382, 1997.
Serreze, M. C., Barrett, A. P., Slater, A. G., Woodgate, R., Aagaard, K., Lammers, R. B., Steele, M., Moritz, R., Meredith, M., and Less, C. M.: The large-scale freshwater cycle of the Arctic, J. Geophys. Res., 111, C11010, 19 pp., doi:10.1029/2005JC003424, 2006.
Shi, J., Zhao, J., Li, S., Cao, Y., and Qu, P.: A double-halocline structure in the Canada Basin of the Arctic Ocean, Acta Oceanol. Sin., 24(6), 25–35, 2005.

Shimada, K., McLaughlin, F., Carmack, E., Proshutinsky, A., Nishino, S., and Itoh, M.: Penetration of the 1990s warm temperature anomaly of Atlantic Water in the Canada Basin, Geophys. Res. Lett., 31, L20301, doi:10.1029/2004GL020860, 2004.

Shimada, K., Itoh, M., Nishino, S., McLaughlin, F., Carmack, E., and Proshutinsky, A.: Halocline structure in the Canada basin of the Arctic Ocean, Geophys. Res. Lett., 32, L03605, doi:10.1029/2004GL021358, 2005.

Smith, J. N., Ellis, K. M., and Boyd, T.: Circulation features in the Central Arctic Ocean revealed by nuclear fuel reprocessing tracers from scientific ice expeditions 1995 and 1996, J. Geophys. Res., 104, 29663–29677, 1999.

Steele, M. and Boyd, T.: Retreat of the cold halocline layer in the Arctic Ocean, J. Geophys. Res., 103(C5), 10419–10435, 1998.

Steele, M., Morison, J., Ermold, W., Rigor, E., and Ortmeyer, M.: Circulation of summer Pacific halocline water in the Arctic Ocean, J. Geophys. Res., 109, C02027, doi:10.1029/2003JC002009, 2004.

Stroeve, J. C., Maslanik, J., Serreze, M. C., Rigor, I., Meier, W., and Fowler, C.: Sea ice response to an extreme negative phase of the Arctic oscillation during winter 2009/2010, Geophys. Res. Lett., 38, L02502, 2011.

Swift, J. H., Jones, E. P., Aagaard, K., Carmack, E. C., Hingston, M., Macdonald, R. W., McLaughlin, F. A., and Perkin, R. G.: Waters of the Makarov and Canada basins, Deep-Sea Res. Pt. II, 44(8), 1503–1529, 1997.

Toole, J. M., Timmermans, M. L., Perovich, D. K., Krishfield, R. A., Proshutinsky, A., and Richter-Menge, J. A.: Influences of the Ocean Surface Mixed layer and thermohaline stratification on Arctic Sea Ice in the Central Canada basin, J. Geophys. Res., 115, C10018, doi:10.1029/2009JC005660, 2010.

Weingartner, T., Aagaard, K., Woodgate, R., Danielson, S., Sasaki, Y., and Cavalieri, D.: Circulation on the North Central Chukchi Sea shelf, Deep-Sea Res. Pt. II, 52, 3150–3174, 2005.

Woodgate, R. A. and Aagaard, K.: Revising the Bering Strait freshwater flux into the Arctic Ocean, Geophys. Res. Lett., 32, L02602, doi:10.1029/2004GL021747, 2005.

Woodgate, R. A., Aagaard, K., Muench, R. D., Gunn, J., Bjork, G., Rudels, B., Roach, A. T., and Schauer, U.: The Arctic Ocean boundary current along the Eurasian slope and adjacent Lomonosov ridge: water mass properties, transports and transformations from moored instruments, Deep-Sea Res. Pt. I, 48, 1757–1792, 2001.

Woodgate, R. A., Aagaard, K., and Weingartner, T. J.: A year in the physical oceanography of the Chukchi Sea: moored measurements from autumn 1990–1991, Deep-Sea Res. Pt. II, 52, 3116–3149, 2005a.
Woodgate, R. A., Aagaard, K., and Weingartner, T. J.: Monthly temperature, salinity, and transport variability of the Bering Strait through flow, Geophys. Res. Lett., 32, L04601, doi:10.1029/2004GL021880, 2005b.
Woodgate, R. A., Aagaard, K., Swift, J. H., Smethie Jr, W. M., and Falkner, K. K.: Atlantic water circulation over the Mendeleev Ridge and Chukchi Borderland from thermohaline intrusions and water mass properties, J. Geophys. Res., 112, C02005, doi:10/1029/2005JC003416, 2007.
Woodgate, R. A., Weingartner, T. J., and Lindsay, R.: The 2007 Bering Strait oceanic heat flux and anomalous Arctic sea ice retreat, Geophys. Res. Lett., 37, L01602, doi:10.1029/2009GL041621, 2010.

OSD
9, 2001–2038, 2012

Hydrographic changes in the Canadian basin during AO inversion

P. Bourgain et al.

Table 1. Number of CTD stations by year and source used for this study.

Year	Source				
	CHINARE	ITP	RV-Polarstern	CCGS-LSSL	TOTAL
2008	63	59	11	71	231
2010	50	22	0	72	182

OSD
9, 2001–2038, 2012

Table 2. Temporal evolution of the NSTM characteristics in the five areas between 2008 and 2010. Note that the average value of NSTM being calculated on a different number of points in 2008 and 2010, the average value of NSTM (2010)–NSTM (2008) is not equal to the difference between the average value of NSTM (2010) and the average value of NSTM (2008). This remark stands for the other variables.

	Temperature (°C)			Depth (dbar)		
	2008	2010	2010–2008	2008	2010	2010–2008
MAP	-1.41 ± 0.19	–	disappearance	25 ± 3	–	disappearance
CaB	-0.17 ± 1.69	-0.78 ± 0.57	-0.91 ± 1.4	16 ± 6	21 ± 5	7 ± 6
ChB	-0.24 ± 0.89	-1.04 ± 0.41	-0.77 ± 0.68	9 ± 3	14 ± 7	5 ± 8
BA	1.60 ± 1.40	0.58 ± 0.55	-1.18 ± 1.60	12 ± 2	7 ± 1	-5 ± 3
MK	3.06 ± 1.83	2.05 ± 2.07	-1.01 ± 1.35	8 ± 2	15 ± 6	7 ± 6

OSD
9, 2001–2038, 2012

Table 3. Temporal evolution of the SPaW characteristics in the five areas between 2008 and 2010.

	PWI (°C)			Depth (dbar)		
	2008	2010	2010–2008	2008	2010	2010–2008
MAP	0.46 ± 0.11	0.35 ± 0.22	0.00 ± 0.18	72 ± 8	62 ± 7	−7 ± 10
CaB	0.93 ± 0.24	1.05 ± 0.19	0.05 ± 0.31	80 ± 8	75 ± 10	−8 ± 10
ChB	0.82 ± 0.25	0.99 ± 0.18	0.17 ± 0.21	68 ± 17	61 ± 9	−8 ± 19
BA	0.91 ± 0.22	1.29 ± 0.23	0.35 ± 0.43	61 ± 6	75 ± 4	14 ± 7
MK	1.09 ± 0.14	0.59 ± 0.27	−0.50 ± 0.23	77 ± 9	66 ± 11	−10 ± 7

OSD

9, 2001–2038, 2012

Table 4. Temporal evolution of the WPaW characteristics in the five areas between 2008 and 2010.

	Temperature (°C)			Depth (dbar)		
	2008	2010	2010–2008	2008	2010	2010–2008
MAP	-1.52 ± 0.04	-1.54 ± 0.04	-0.01 ± 0.04	110 ± 24	85 ± 25	-9 ± 30
CaB	-1.49 ± 0.06	-1.54 ± 0.03	-0.04 ± 0.08	163 ± 24	181 ± 12	14 ± 18
ChB	-1.58 ± 0.03	-1.56 ± 0.03	0.02 ± 0.05	145 ± 26	165 ± 19	19 ± 14
BA	-1.57 ± 0.04	-1.51 ± 0.03	0.07 ± 0.03	143 ± 20	174 ± 7	26 ± 20
MK	-1.49 ± 0.02	-1.42 ± 0.03	0.07 ± 0.03	150 ± 25	147 ± 18	-3 ± 11

Table 5. Temporal evolution of the AW characteristics in the five areas between 2008 and 2010.

	Temperature (°C)			Depth (dbar)		
	2008	2010	2010–2008	2008	2010	2010–2008
MAP	0.79 ± 0.06	0.89 ± 0.04	0.07 ± 0.06	376 ± 31	377 ± 31	3 ± 23
CaB	0.82 ± 0.05	0.80 ± 0.04	−0.02 ± 0.03	421 ± 23	448 ± 13	18 ± 13
ChB	0.88 ± 0.03	0.84 ± 0.04	−0.04 ± 0.03	433 ± 20	443 ± 16	9 ± 15
BA	0.69 ± 0.06	0.70 ± 0.09	0 ± 0.04	385 ± 39	431 ± 20	42 ± 26
MK	0.59 ± 0.07	0.61 ± 0.09	0.02 ± 0.03	428 ± 18	409 ± 15	−18 ± 17

OSD
9, 2001–2038, 2012

Table 6. Temporal evolution of the H_{FW} (m) in the five areas between 2008 and 2010.

	2008	2010	2010–2008
MAP	13.92 ± 2.53	9.54 ± 2.44	−2.78 ± 3.18
CaB	20.82 ± 3.05	23.63 ± 2.97	1.89 ± 1.35
ChB	17.01 ± 2.83	18.91 ± 2.90	1.89 ± 1.36
BA	16.88 ± 2.65	20.25 ± 2.44	3.04 ± 1.26
MK	21.87 ± 3.54	18.19 ± 3.73	−3.52 ± 1.40

OSD
9, 2001–2038, 2012

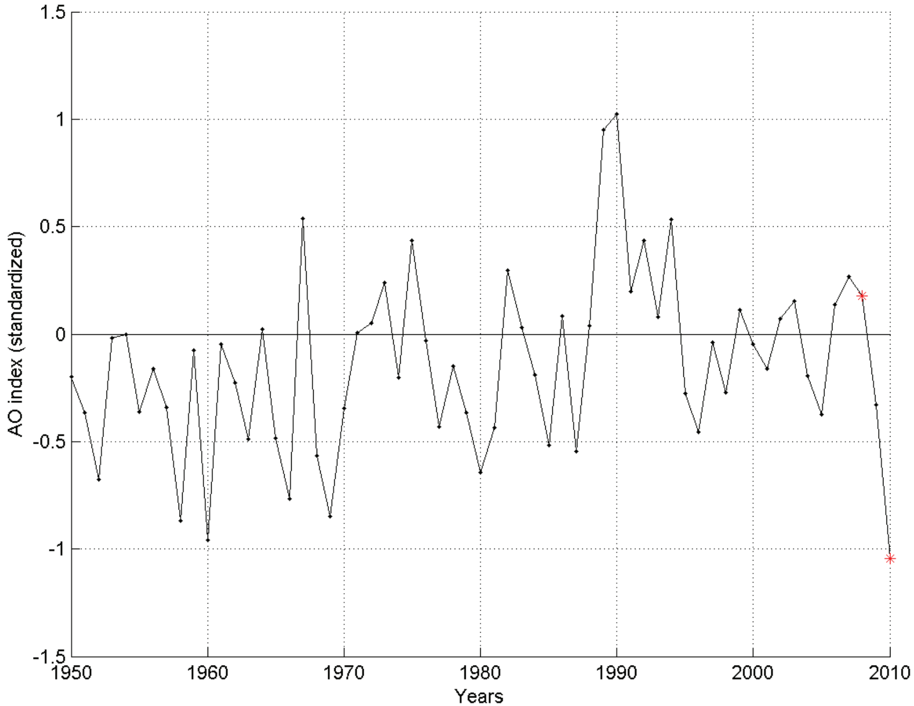

Fig. 1. Time series of the annually-averaged Arctic Oscillation Index for the period 1950–2006 standardized yearly (1979–2000 base period) and based on data from the NCEP website. Years 2008 and 2010 are indicated in red.

OSD
9, 2001–2038, 2012

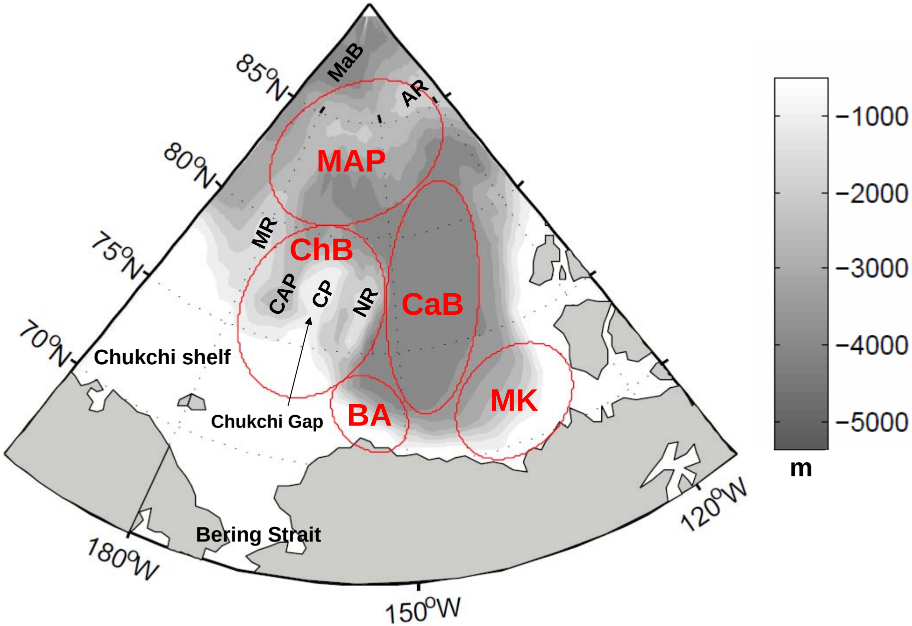

Fig. 2. Bathymetry and main topographic features of the Canadian basin. CP stands for Chukchi Plateau, NR for Northwind Ridge, and CAP for Chukchi Abyssal Plain. AR and MR stand for Alpha Ridge and Mendeleyev Ridge, respectively, and MaB stands for the Makarov basin. The ellipses correspond to the five subdivisions of the area chosen for this study: the Chukchi borderland (ChB including the CP, the NR and the CAP), the Barrow canyon region (BA), the Mackenzie River region (MK), the Canada basin (CaB), the Mendeleyev Abyssal Plain (MAP). The colorbar indicates the bathymetry in meters.

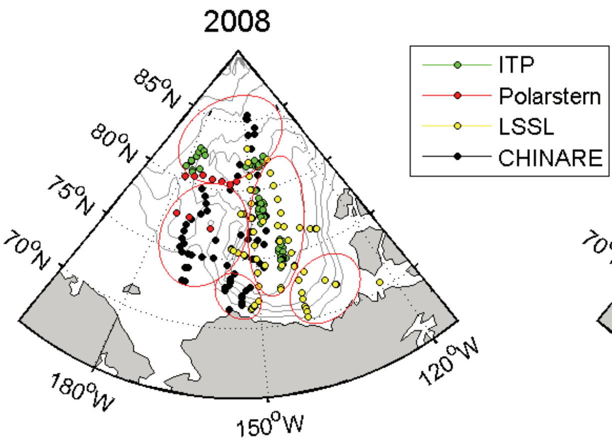

Fig. 3. Location and source of the data for years 2008 (left) and 2010 (right). The ellipses correspond to the subdivision chosen for the Canadian basin.

OSD
9, 2001–2038, 2012

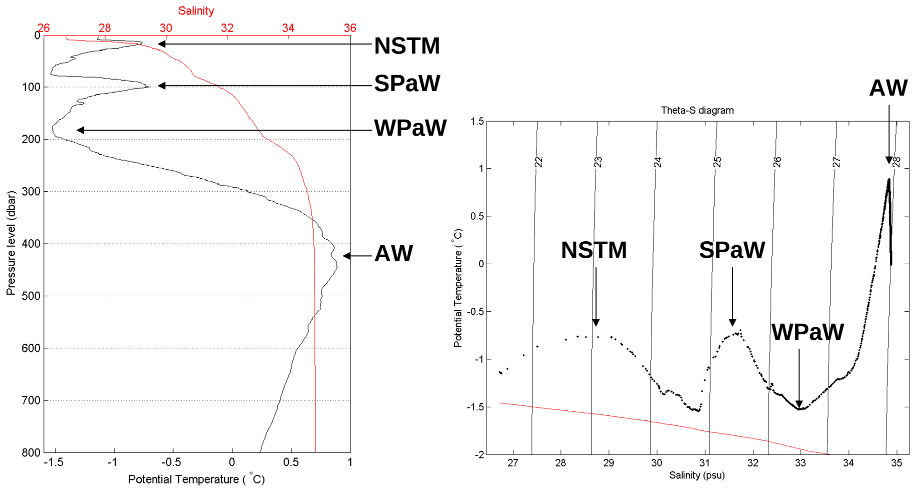

Fig. 4. A typical vertical potential temperature and salinity profile of the study area (left) and the corresponding θS diagram (right) with the freezing point indicated in red. The NSTM (Near Surface Temperature Maximum), the SPaW (Summer Pacific water), the WPaW (Winter Pacific water) and the AW (Atlantic water) are indicated. This profile was recorded in August 2008 during the CHINARE campaign, at location (76.98° N, 146.1° W).

OSD
9, 2001–2038, 2012

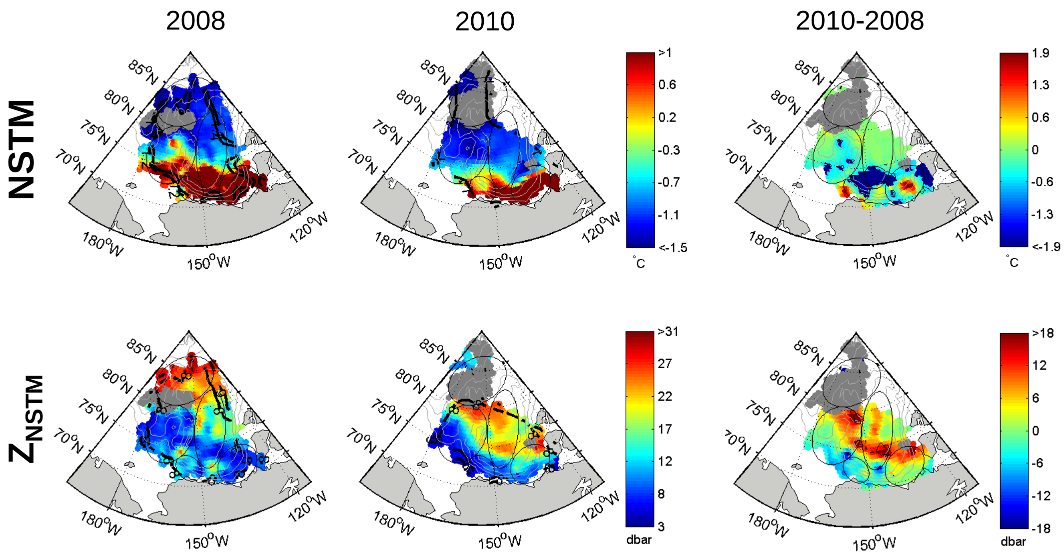

Fig. 5. Kriging interpolation of the Near Surface Temperature Maximum (NSTM, top) and its depth level (Z_{NSTM}, bottom), for years 2008 (left panel) and 2010 (middle panel), and the evolution between the two years (right panel). Grey areas correspond to the absence of the NSTM. On the left and middle panels, thick black dashed isolines correspond to estimation error (σ) due to Kriging interpolation process. The isolines represented are $\sigma = 1\,^{\circ}$C and $\sigma = 1.2\,^{\circ}$C for NSTM, and $\sigma = 8$ dbar and $\sigma = 9$ dbar for Z_{NSTM}. On the right panel, thin black isolines correspond to 95 % significance.

OSD
9, 2001–2038, 2012

Hydrographic changes in the Canadian basin during AO inversion

P. Bourgain et al.

OSD
9, 2001–2038, 2012

Hydrographic changes in the Canadian basin during AO inversion

P. Bourgain et al.

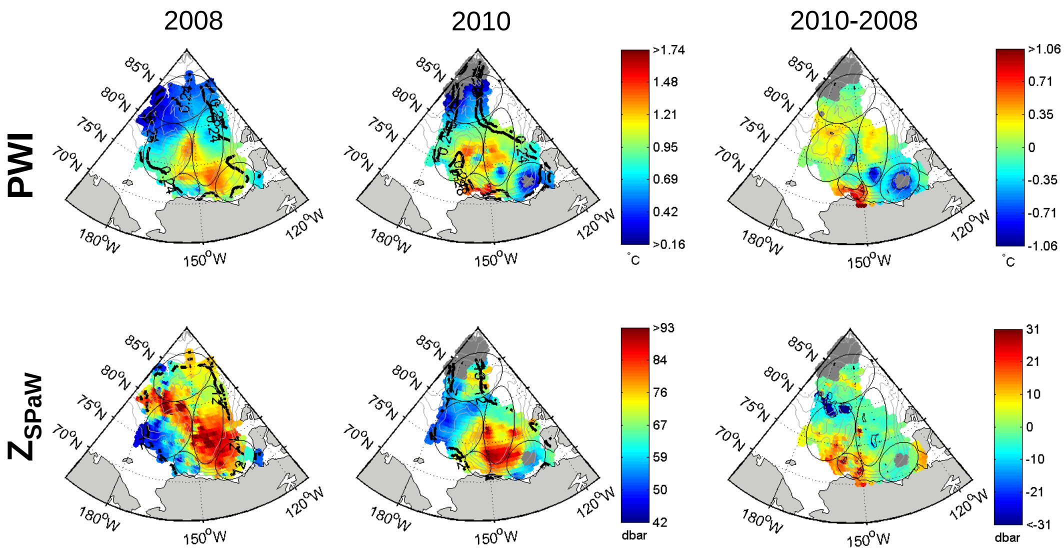

Fig. 6. Kriging interpolation of PWI (PWI = $T_{SPaW} - T_{FP}$, top) and its depth level (Z_{SPaW}, bottom), for years 2008 (left panel) and 2010 (middle panel), and the evolution between the two years (right panel). Grey areas correspond to the absence of the SPaW. On the left and middle panels, thick black dashed isolines correspond to estimation error (σ) due to Kriging interpolation process. The isolines represented are σ = 0.24 °C and σ = 0.28 °C for PWI, and σ = 12 dbar and σ = 13 dbar for Z_{SPaW}. On the right panel, thin black isolines correspond to 95 % significance.

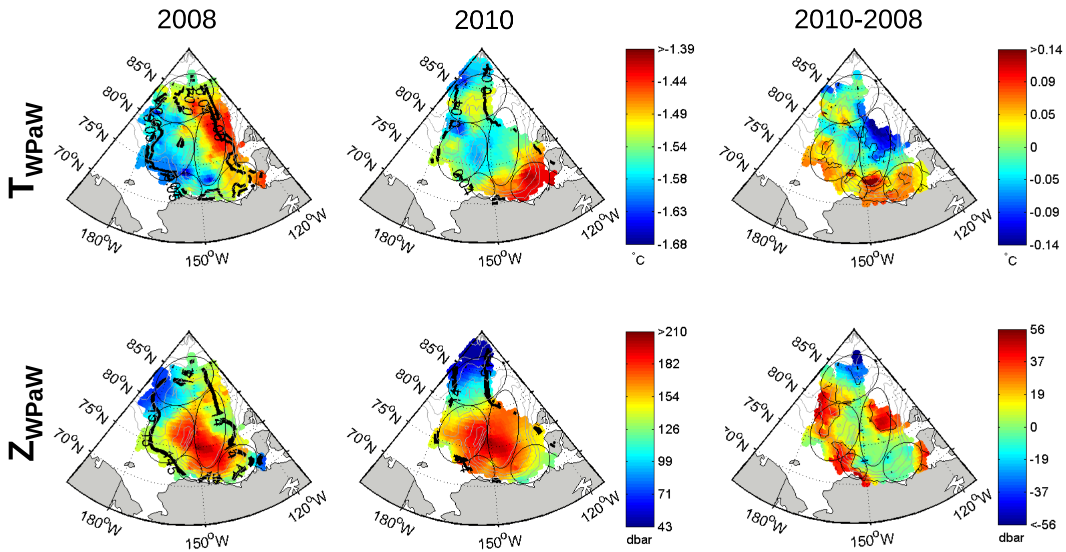

Fig. 7. Kriging interpolation of the WPaW temperature (T_{WPaW}, top) and the depth level (Z_{WPaW}, bottom), for years 2008 (left panel) and 2010 (middle panel), and the evolution between the two years (right panel). On the left and middle panels, thick black dashed isolines correspond to estimation error (σ) due to Kriging interpolation process. The isolines represented are σ = 0.04 °C and σ = 0.05 °C for T_{WPaW}, and σ = 14 dbar and σ = 15 dbar for Z_{WPaW}. On the right panel, thin black isolines correspond to 95 % significance.

OSD
9, 2001–2038, 2012

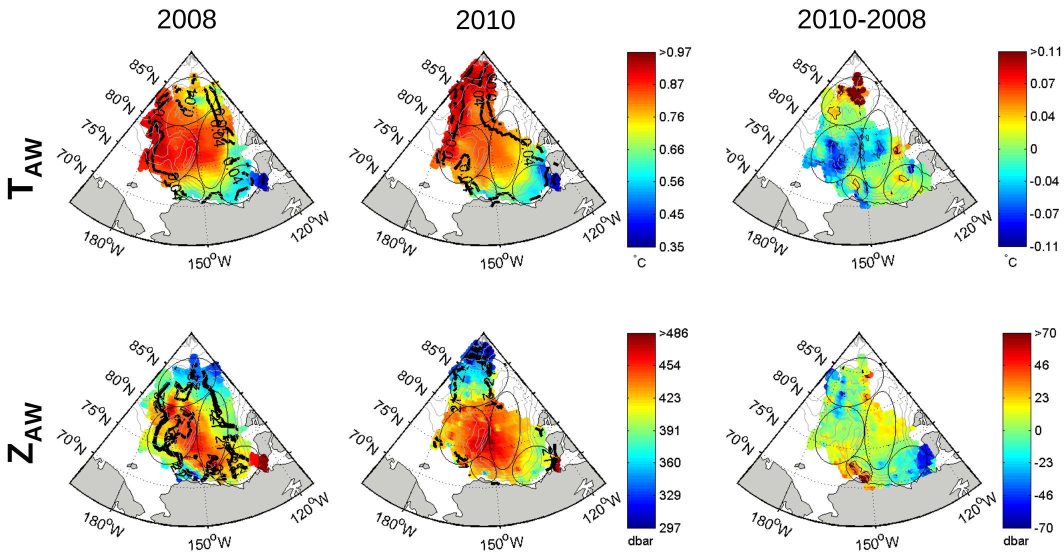

Fig. 8. Kriging interpolation of the AW core temperature (T_{AW}, top) and its depth level (Z_{AW}, bottom), for years 2008 (left panel) and 2010 (middle panel), and the evolution between the two years (right panel). On the left and middle panels, thick black dashed isolines correspond to estimation error (σ) due to Kriging interpolation process. The isolines represented are σ = 0.04 °C and σ = 0.05 °C for T_{AW}, and σ = 21 dbar and σ = 22 dbar for Z_{AW}. On the right panel, thin black isolines correspond to 95 % significance.

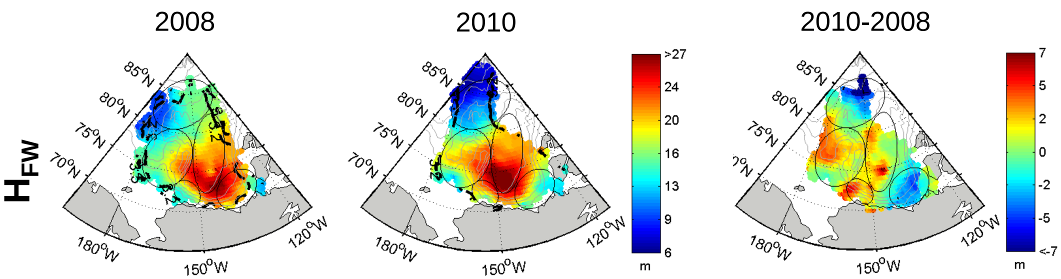

Fig. 9. Kriging interpolation of H_{FW}, the liquid freshwater content, for years 2008 (left panel) and 2010 (middle panel), and the evolution between the two years (right panel). On the left and middle panels, thick black dashed isolines correspond to estimation error (σ) due to Kriging interpolation process. The isolines represented are $\sigma = 3.2$ m and $\sigma = 3.5$ m. On the right panel, thin black isolines correspond to 95 % significance.

OSD
9, 2001–2038, 2012

Hydrographic changes in the Canadian basin during AO inversion

P. Bourgain et al.